

Neutrino Oscillations in Finite Time Path Out-of-Equilibrium Thermal Field Theory

Dadić, Ivan; Klabučar, Dubravko

Source / Izvornik: **Symmetry, 2023, 15**

Journal article, Published version

Rad u časopisu, Objavljena verzija rada (izdavačev PDF)

<https://doi.org/10.3390/sym15111970>

Permanent link / Trajna poveznica: <https://urn.nsk.hr/urn:nbn:hr:217:596605>

Rights / Prava: [Attribution 4.0 International](#)/[Imenovanje 4.0 međunarodna](#)

Download date / Datum preuzimanja: **2024-08-29**




Repository / Repozitorij:

[Repository of the Faculty of Science - University of Zagreb](#)



Article

Neutrino Oscillations in Finite Time Path Out-of-Equilibrium Thermal Field Theory

Ivan Dadić¹ and Dubravko Klabučar^{2,*} ¹ Rudjer Bošković Institute, Bijenička cesta 54, 10000 Zagreb, Croatia; ivan.dadic@irb.hr² Physics Department, Faculty of Science, University of Zagreb, Bijenička cesta 32, 10000 Zagreb, Croatia

* Correspondence: klabucar@phy.hr

Abstract: We demonstrate that the Finite-Time-Path Field Theory is an adequate tool for calculating neutrino oscillations. We apply this theory using a mass-mixing Lagrangian which involves the correct Dirac spin and chirality structure and a Pontecorvo–Maki–Nakagawa–Sakata (PMNS)-like mixing matrix. The model is exactly solvable. The Dyson–Schwinger equations transform propagators of the input free (massless) flavor neutrinos into a linear combination of oscillating (massive) neutrinos. The results are consistent with the predictions of the PMNS matrix while allowing for extrapolation to early times.

Keywords: neutrino; oscillation; finite-time path; quantum field theory

1. Introduction

The evidence for neutrino oscillations, which solve the solar neutrino problem [1], started with the study of atmospheric oscillations [2]. Evidence has been collected from various sources and for various distances from the sources over a wide range of neutrino energies and detectors [3–43].

Neutrino oscillations, as well as similar problems such as kaon oscillations and decays, suffer from the absence of a proper formalism for the features in which a finite-time description is essential.

The most important aspect of this paper is to demonstrate that the Finite Time Path Field Theory (FTPFT) is an adequate tool [44,45] to treat such problems. In particular, we start with the free Lagrangian \mathcal{L}_0 of massless neutrinos with three flavors; however, we mix them dynamically through an interaction Lagrangian \mathcal{L}_I , as in addition to the standard weak interaction term \mathcal{L}_W it has the term \mathcal{L}_{Mix} , which contains a Pontecorvo–Maki–Nakagawa–Sakata (PMNS)-like matrix involving neutrino masses. The term \mathcal{L}_W is of course crucial for the processes of creation and detection of flavor neutrinos. Nevertheless, we adopt the approximation where the neutrino mixing is fully due to the term \mathcal{L}_{Mix} , that is, we neglect the residual influence of \mathcal{L}_W on the neutrino masses and mixing. Of course, we must keep in mind the caveat that not calculating these corrections misses the contributions from the vacuum condensate, which Blasone et al. [46–48] found to be important corrections to the PMNS result. Nevertheless, they vanish in the relativistic limit, while the PMNS result is recovered [46–48]. Because the case of nonrelativistic neutrino kinematics seems to be far from present experimental capabilities, we proceed to study neutrino propagators in our aforescribed framework, which provides us with an exactly solvable model suitable for studying how FTPFT can be applied to neutrino oscillations.

Through the exact solution of the Dyson–Schwinger equations (DSE), we then obtain propagators (with the retarded S_R and advanced S_A components) of oscillating (massive) neutrinos which couple to the weak interactions. The DSE equation for the Keldysh component (S_K) of neutrino propagators leads to two possible histories distinguished by two of three masses (say, m_i and m_j) for which the interference leads to oscillations. An equal time limit of S_K provides the number of neutrinos at time t .



Citation: Dadić, I.; Klabučar, D. Neutrino Oscillations in Finite Time Path Out-of-Equilibrium Thermal Field Theory. *Symmetry* **2023**, *15*, 1970. <https://doi.org/10.3390/sym15111970>

Academic Editor: Charalampos Moustakidis

Received: 3 July 2023

Revised: 11 September 2023

Accepted: 21 September 2023

Published: 24 October 2023



Copyright: © 2023 by the authors. Licensee MDPI, Basel, Switzerland. This article is an open access article distributed under the terms and conditions of the Creative Commons Attribution (CC BY) license (<https://creativecommons.org/licenses/by/4.0/>).

The origin of neutrino masses has not yet been answered conclusively. The variety of extant approaches includes the Majorana mass term, right-handed neutrinos with a see-saw mechanism, supersymmetric extensions of Standard model, and more. One intriguing possibility is the generation of neutrino masses and mixing via the aforementioned flavor vacuum condensate [46–48]. However, in the present paper we do not address the issue of the origin of neutrino masses, and focus on demonstrating the calculation of neutrino oscillations in the FTPFT framework.

Whatever the mechanism of neutrino mass generation, in this paper we assume that it manifests itself through an additional term in the Lagrangian: the mass mixing term \mathcal{L}_{Mix} . Here, the interaction Lagrangian contains the mass mixing matrix in a close analogy to the PMNS matrix except with an explicit Dirac spin and chirality structure. The model is exactly solvable.

To calculate neutrino oscillations, we use FTPFT; [49,50] in addition, see [51–68], often called the closed time path (CTP) thermal field theory (TFT). We find this to be an appropriate tool for calculating a wide variety of problems, including equilibrium and nonequilibrium TFT problems, for which it was originally constructed [49,50], as well as scattering processes, decays, and oscillations.

How can field theory describe oscillations? It depends on which version of field theory is employed (for example, see [69,70] and references therein). If we look at the predominant field theory approach, namely, the S-matrix approach, it exhibits excellent properties: adiabatic switching of interaction, Gell-Mann–Low (G-L) theorem, Fermi’s golden rule, reduction technique, renormalization, etc. However, for time-dependent processes, notably oscillations, it has nothing to say, in the sense that it includes adiabatic switching (on and off) of the interaction and acts between the infinite initial time $t_i = -\infty$ and final time $t_f = \infty$.

FTPFT, on the other hand, uses a finite time path, no adiabatic switching, and no G-L theorem. The particle states are not exactly the eigenstates of the full Hamiltonian. Renormalization, as we have indicated in [67,68], is somewhat more involved; nevertheless, it can be performed in finite time with essentially the same technique of dimensional regularization.

The drawback of this theory is the lack of a Gell-Mann–Low-type theorem. Nevertheless, FTPFT does not contain disconnected subdiagrams owing to the absence of the maximal-time vertices [61,62,64]. Thus, this drawback may be cured after carrying out all of the calculations in a proper way by considering the large time behavior of the contributions. Then, in this limit one can expect the G-L theorem to again be valid.

The particle number is obtained as the equal time limit (ETL) of the re-summed S_K propagator (or better) as the average of ETL (AETL) for the contributions distinguished by $t_{1f} - t_{2f}$ (see Appendix A, especially Appendix A.7). These processes contribute inclusively to the particle number. Fermi’s golden rule need not be put in by hand, as it emerges naturally during calculation of the convolution products (*-products).

In certain applications, the solution of DSE can be written in a closed form. The solution of DSE is illustrative: conserving energy and momentum along the chain, the chain of retarded functions extends from the final time t towards the earliest time $t_{min} \geq 0$. There, it meets a S_K propagator containing the initial distribution function. At that time, there is a (single) convolution product, which does not conserve energy. Instead, it creates just enough oscillating deviations from the energy-conserving value to satisfy the uncertainty relations. From the lowest time, another chain of advanced functions progresses back to the final time. It conserves energy and momentum as well; however, the energy of the advanced chain differs from the energy of the retarded chain. With the help of this energy difference, the convolution product creates oscillations. It is easy to see that with increasing time the uncertainty in energy becomes smaller, which is in the full agreement with the uncertainty relations.

In certain special cases, energy is conserved at the remaining *-product. For instance, this is the case when Fermi’s golden rule emerges.

The remainder of this paper is organized as follows: first, we provide a short overview of the PMNS-approach; then, we define the dynamics of our approach through the mass mixing interaction Lagrangian \mathcal{L}_{Mix} (9).

Our calculation is based on the DSE (12)–(15) and their closed form solution. This solution defines the oscillating neutrino which possesses flavor as massive and weakly interacting.

The equal time limit of the S_K propagator is directly connected to the neutrino number, as it is measured at time t . In the process of calculation, we show how the number of complicated $*$ -products appearing in the formal solution simplifies to a single $*$ -product, which is necessary for the time evolution and energy–time uncertainty relations.

As a result of this calculation, we obtain the neutrino number at time t . Projection to the flavor degree of freedom exhibits oscillating behavior. This result is consistent with Heisenberg’s uncertainty relations between time and energy. We reproduce the PMNS result exactly within the limit of ultrarelativistic neutrinos and large time.

Finally, we discuss prospects for further research.

Further details and calculation can be found in Appendix A.

2. PMNS Theory of Neutrino Oscillation

In the PMNS theory of neutrino oscillation [71–75], three flavor neutrino states that interact weakly are mixed to three different superpositions of the neutrino states of definite mass (for mixing in gauge theories, see [6]). In the flavor states, neutrinos are emitted and absorbed through weak processes; however, they travel as mass eigenstates.

This is mathematically expressed as

$$|v_\alpha\rangle = \sum_i U_{\alpha i} |v_i\rangle, \quad |v_i\rangle = \sum_\alpha U_{\alpha i}^* |v_\alpha\rangle, \quad (1)$$

where $\alpha = e, \mu, \tau$ are the flavor indices, respectively, e -electron neutrinos, μ -muon neutrinos, and τ -taunon neutrinos, that label neutrinos with definite flavors, while m_i , $i = 1, 2, 3$, are the indices of the neutrino mass states. To describe antineutrinos, it is necessary to use complex-conjugate matrices $U_{\alpha i} \leftrightarrow U_{\alpha i}^*$. The matrix $U_{\alpha i}$ is the PMNS-matrix, introduced in a way analogous to the CKM matrix describing the mixing of quarks.

The size of the matrix depends on theory. For the standard three-neutrino theory, the matrix is 3×3 . For more neutrinos (including sterile ones), the matrix could be larger. There are anomalies [4,5,76–86], suggesting that the model requires further refinement.

The 3×3 PMNS matrix (2), for example, is provided in [22]:

$$U = \begin{pmatrix} U_{e1} & U_{e2} & U_{e3} \\ U_{\mu1} & U_{\mu2} & U_{\mu3} \\ U_{\tau1} & U_{\tau2} & U_{\tau3} \end{pmatrix} \quad (2)$$

$$= \begin{pmatrix} 1 & 0 & 0 \\ 0 & c_{23} & s_{23} \\ 0 & -s_{23} & c_{23} \end{pmatrix} \begin{pmatrix} c_{13} & 0 & s_{13}e^{-i\delta} \\ 0 & 1 & 0 \\ -s_{13}e^{i\delta} & 0 & c_{13} \end{pmatrix} \begin{pmatrix} c_{12} & s_{12} & 0 \\ -s_{12} & c_{12} & 0 \\ 0 & 0 & 1 \end{pmatrix} \begin{pmatrix} e^{i\alpha_1/2} & 0 & 0 \\ 0 & e^{i\alpha_2/2} & 0 \\ 0 & 0 & 1 \end{pmatrix},$$

where $c_{ij} = \cos \theta_{ij}$ and $s_{ij} = \sin \theta_{ij}$. The phase factors α_1 and α_2 are relevant only if the neutrinos are Majorana particles, i.e., if the neutrino is identical to its antineutrino, otherwise they can be ignored. The phase factor δ measures the degree of violation of CP symmetry, which has not yet been observed experimentally.

Note that Relation (1) is valid only approximately, as particles with the same energy and momentum but different masses cannot simultaneously be on the mass shell. The same feature appears in the usual treatment of neutrino oscillations in field theory, where it is known as mass-shell approximation [69,70,87,88].

A neutrino travels through space as a massive neutrino. Its time evolution is described (in units $c = 1, \hbar = 1$) by $|v_i(t)\rangle = e^{-i(E_i t - \vec{p}_i \cdot \vec{x})} |v_i(0)\rangle$ for each mass- and energy-eigenstate

$|\nu_i\rangle$ with mass m_i and eigenenergy $E_i = \sqrt{p_i^2 + m_i^2}$. However, weak processes actually produce flavor states $|\nu_\alpha\rangle$, which are, in accordance with Equation (1), superpositions of these mass- and energy-eigenstates $|\nu_i\rangle$. Due to their energy differences $E_i - E_j$, such superpositions have an energy uncertainty ΔE (5).

In the quantum mechanical treatment of neutrino oscillations, it is standard to assume (for example, see [89,90]) that all mass eigenstates $|\nu_i\rangle$ have the same momentum, i.e., their energies E_i differ by their masses m_i and the flavor neutrino state $|\nu_\alpha\rangle$ is determined by the momentum.

In the ultrarelativistic limit, $|\vec{p}_i| = p_i \gg m_i$. Thus, $p_i \approx E$, the neutrino energy in the limit $m_i \rightarrow 0$, such that $\forall i$:

$$E_i \simeq p_i + \frac{m_i^2}{2p_i} \approx E + \frac{m_i^2}{2E}, \quad \text{and} \quad t \approx L, \quad (3)$$

where t is the time from the beginning of evolution and L is the distance traveled.

In the process of measurement, the neutrino is projected back to the flavor states. The probability that the initial neutrino with flavor α will be detected later as having flavor β is defined as

$$P_{\alpha \rightarrow \beta} = |\langle \nu_\beta(L) | \nu_\alpha \rangle|^2 = \left| \sum_i U_{\alpha i}^* U_{\beta i} e^{-i \frac{m_i^2 L}{2E}} \right|^2.$$

This can be written as

$$\begin{aligned} P_{\alpha \rightarrow \beta} &= \delta_{\alpha\beta} - 4 \sum_{i>j} \text{Re} \left(U_{\alpha i}^* U_{\beta i} U_{\alpha j} U_{\beta j}^* \right) \sin^2 \left(\frac{\Delta m_{ij}^2 L}{4E} \right) \\ &+ 2 \sum_{i>j} \text{Im} \left(U_{\alpha i}^* U_{\beta i} U_{\alpha j} U_{\beta j}^* \right) \sin \left(\frac{\Delta m_{ij}^2 L}{2E} \right), \end{aligned} \quad (4)$$

where $\Delta m_{ij}^2 \equiv m_i^2 - m_j^2$.

The second term is related to CP asymmetry:

$$A_{CP}^{(\alpha\beta)} = P(\nu_\alpha \rightarrow \nu_\beta) - P(\bar{\nu}_\alpha \rightarrow \bar{\nu}_\beta) = 4 \sum_{i>j} \text{Im} \left(U_{\alpha i}^* U_{\beta i} U_{\alpha j} U_{\beta j}^* \right) \sin \left(\frac{\Delta m_{ij}^2 L}{2E} \right).$$

With the help of the Jarlskog invariant $\text{Im} \left(U_{\alpha i} U_{\beta i}^* U_{\alpha j} U_{\beta j} \right) = J \sum_{\gamma,k} \varepsilon_{\alpha\beta\gamma} \varepsilon_{ijk}$, the CP asymmetry is expressed as

$$A_{CP}^{(\alpha\beta)} = 16J \sum_{\gamma} \varepsilon_{\alpha\beta\gamma} \sin \left(\frac{\Delta m_{21}^2 L}{4E} \right) \sin \left(\frac{\Delta m_{32}^2 L}{4E} \right) \sin \left(\frac{\Delta m_{31}^2 L}{4E} \right).$$

Note that CP asymmetry in neutrino oscillations has not yet been observed.

Because

$$\Delta E \leq \max_{i,j=1,2,3} (E_i - E_j) \approx \frac{m_i^2 - m_j^2}{2E}, \quad (5)$$

Equation (4) satisfies the time–energy uncertainty relation $\Delta E \Delta t \gtrsim 1$ of Heisenberg (and of Mandelstam and Tamm, as discussed in [90]) for

$$t \gtrsim \frac{2E}{\Delta m_{ij}^2}. \quad (6)$$

For times shorter than (6), the uncertainty relations are fulfilled with the help of neutrino production processes. Specifically, they produce the flavor states $|\nu_\alpha\rangle$, which are

superpositions (1) of $|v_i\rangle$, the eigenstates of neutrino masses m_i , which are so close that they cannot be resolved in a time shorter than (6) [90].

The ultrarelativistic limit applies to all currently observed neutrinos, as it is known that the differences of their squared masses are of the order 10^{-4} eV^2 and their energies are at least 1 MeV. Measured oscillation distances L are on the order of kilometers.

3. Neutrino Oscillation as a Dynamical Process

3.1. The Mass Mixing Term in the Interaction Lagrangian

In order to treat neutrino oscillation as a dynamical process, we start with the neutrino mixing interaction \mathcal{L}_{Mix} of the Dirac spinor Lagrangian, defined by:

$$\mathcal{L}_0(x) = \sum_{\alpha} \bar{\nu}_{\alpha}(x) i \not{\partial} \nu_{\alpha}(x) \quad (7)$$

$$\mathcal{L}_I = \mathcal{L}_W + \mathcal{L}_{Mix} \quad (8)$$

$$\mathcal{L}_{Mix}(x) = \sum_{\alpha,i} \bar{\nu}_{\alpha}(x) U_{\alpha,i}^* M_{ij} U_{\beta,j} \nu_{\beta}(x) + \text{antineutrinos} \quad (9)$$

$$M = \begin{pmatrix} m_1 & 0 & 0 \\ 0 & m_2 & 0 \\ 0 & 0 & m_3 \end{pmatrix}, \quad (10)$$

where $U_{\alpha,i}$ is a 3×3 matrix analogous to the PMNS-matrix. Here, ν_{α} are neutrino spinor wave functions for flavor α and m_i represents the propagating neutrino masses. The initial conditions are fixed through the neutrino distribution function (including either the chirality or a handedness projection operator) which are built in the $S_{f,K}$ component of the flavor neutrino propagator. The massless chiral "flavor neutrinos" (with propagators $S_f(p)$ and weak interaction) enter the DSE. The self-energy is identified from the next-to-lowest order to the DSE through the use of (9) and (10), and is simply the constant matrix

$$\Sigma_{\alpha,\beta} = \Sigma_{\alpha,\beta,R} = \Sigma_{\alpha,\beta,A} = -U_{\alpha,i}^* M_{ij} U_{\beta,j}, \quad \Sigma_{\alpha,\beta,K} = 0 \quad (11)$$

The DSE for fermions and their formal solutions are provided in Appendix A, specifically, (A15)–(A19).

The DSEs for oscillating neutrinos are

$$\tilde{S}_{\beta,\alpha,R} = S_{\beta,R} \delta_{\beta,\alpha} + i S_{\beta,R} * \Sigma_{\beta,\eta,R} * \tilde{S}_{\eta,\alpha,R} \quad (12)$$

$$\tilde{S}_{\beta,\alpha,A} = S_{\beta,A} \delta_{\beta,\alpha} + i S_{\beta,\eta,R} * \Sigma_{\eta,\zeta,A} * \tilde{S}_{\zeta,\alpha,A} \quad (13)$$

$$\tilde{S}_{\beta,\alpha,K} = S_{\beta,K} \delta_{\beta,\alpha} + i [S_{\beta,\eta,R} * \Sigma_{\eta,\zeta,R} * \tilde{S}_{\zeta,\alpha,K} \quad (14)$$

$$+ S_{\beta,\eta,K} * \Sigma_{\eta,\zeta,A} * \tilde{S}_{\zeta,\alpha,A} + S_{\beta,\eta,R} * \Sigma_{\eta,\zeta,K} * \tilde{S}_{\zeta,\alpha,A}], \quad (15)$$

where S denotes the lowest-order Green function and the same symbol with a tilde (\tilde{S}) denotes the corresponding re-summed Green function, as explained in Appendix A.6.

3.2. Solution of the Dyson–Schwinger Equations for Oscillating Neutrinos

The formal solution for (12)–(15) is

$$\tilde{S}_{\beta,\alpha,R} = [1 - i S_R * \Sigma_R]_{\beta,\eta}^{-1} * S_{\eta,\alpha,R} = S_{\beta,\eta,R} * [1 - i \Sigma_R * S_R]_{\eta,\alpha}^{-1},$$

$$\tilde{S}_{\beta,\alpha,A} = [1 - i S_A * \Sigma_A]_{\beta,\eta}^{-1} * S_{\eta,\alpha,A} = S_{\beta,\eta,A} * [1 - i \Sigma_A * S_A]_{\eta,\alpha}^{-1},$$

$$\tilde{S}_{\beta,\alpha,K} = -S_{\beta,\eta,K,A} * (1 - i \Sigma_A * S_A)_{\eta,\alpha}^{-1} + (1 - i S_R * \Sigma_R)_{\beta,\eta}^{-1} * S_{\eta,\alpha,K,R}$$

$$\begin{aligned}
 &+i(1 - iS_R * \Sigma_R)_{\beta,\eta}^{-1} * [S_{\eta,\zeta,R} * \Sigma_{\zeta,\omega,K} * S_{\omega,\theta,A} - S_{\eta,\zeta,R} * \Sigma_{\zeta,\omega,R} * S_{\omega,\theta,K,A} \\
 &+ S_{\eta,\zeta,K,R} * \Sigma_{\zeta,\omega,A} * S_{\omega,\theta,A}] * (1 - i\Sigma_A * S_A)_{\theta,\alpha}^{-1}. \tag{16}
 \end{aligned}$$

The solution simplifies owing to the following three reasons:

1. The self-energy is a simple matrix, not a retarded or advanced function;
2. The *-products among the bare propagators turn to algebraic products except for the case where one factor is retarded (R or K,R) and the other is advanced (A or K,A);
3. The matrix U is unitary.

Next, we calculate $(1 - i\Sigma_{R(A)} * S_{R(A)})_{\theta,\alpha}^{-1}$; the matrix inversion is simple, and we obtain

$$(1 - i\Sigma * S_R)_{\beta,\alpha}^{-1}(p) = \sum_i U_{\beta,i}^* \frac{p^2 + m_i \not{p}}{p^2 - m_i^2 + ip_0\epsilon} U_{\alpha,i}. \tag{17}$$

Then, we obtain the re-summed retarded propagator component:

$$\tilde{S}_{\beta,\alpha,R}(p) = (1 - i\Sigma * S_R)_{\beta,\eta}^{-1} S_{\eta,\alpha,R}(p) = \sum_i U_{\beta,i}^* \frac{-i(m_i + \not{p})}{p^2 - m_i^2 + ip_0\epsilon} U_{\alpha,i} \tag{18}$$

and the resummed advanced propagator component

$$\tilde{S}_{\beta,\alpha,A}(p) = (1 - i\Sigma * S_A)_{\beta,\eta}^{-1} S_{\eta,\alpha,A}(p) = \sum_i U_{\beta,i}^* \frac{-i(m_i + \not{p})}{p^2 - m_i^2 - ip_0\epsilon} U_{\alpha,i}. \tag{19}$$

We now have an important conclusion. Relations (18) and (19) express the re-summed flavor propagator through the linear combination of “propagating” neutrino propagators. This should be contrasted to the “similar” (mathematically ill-defined) relations between wave functions of flavor and propagating neutrinos.

Now, we turn to the $\tilde{S}_{\beta,\alpha,K}$ propagator. Insertion of (17)–(19) into (16) provides us with

$$\begin{aligned}
 \tilde{S}_{\beta,\alpha,K} &= -\delta_{f,\alpha} \sum_i U_{\beta,i}^* U_{\alpha,i} \frac{i}{p^2 - m_i^2 - ip_0\epsilon} \\
 &\times \{ [1 - 2n_f(\vec{p})] \frac{p_0 + |\vec{p}|}{2|\vec{p}|} (\gamma_0|\vec{p}| - \vec{\gamma}\vec{p}) - [1 - 2n_{\bar{f}}(-\vec{p})] \frac{p_0 - |\vec{p}|}{2|\vec{p}|} (\gamma_0|\vec{p}| + \vec{\gamma}\vec{p}) \} \frac{1 - \gamma_5}{2} \\
 &+ \delta_{\beta,f} \sum_i U_{\beta,i}^* U_{\alpha,i} \frac{i}{p^2 - m_i^2 + ip_0\epsilon} \\
 &\times \{ [1 - 2n_f(\vec{p})] \frac{p_0 + |\vec{p}|}{2|\vec{p}|} (\gamma_0|\vec{p}| - \vec{\gamma}\vec{p}) - [1 - 2n_{\bar{f}}(-\vec{p})] \frac{p_0 - |\vec{p}|}{2|\vec{p}|} (\gamma_0|\vec{p}| + \vec{\gamma}\vec{p}) \} \frac{1 - \gamma_5}{2} \\
 &+ i\delta_{f,\alpha} \sum_{i,j} U_{\beta,i}^* \frac{p^2 + m_i \not{p}}{(p^2 - m_i^2 + ip_0\epsilon)(p^2 + ip_0\epsilon)} U_{\alpha,i} [-im_i(-i\not{p})] \\
 &* \{ [1 - 2n_f(\vec{p})] \frac{p_0 + |\vec{p}|}{2|\vec{p}|} (\gamma_0|\vec{p}| - \vec{\gamma}\vec{p}) \\
 &- [1 - 2n_{\bar{f}}(-\vec{p})] \frac{p_0 - |\vec{p}|}{2|\vec{p}|} (\gamma_0|\vec{p}| + \vec{\gamma}\vec{p}) \} \frac{1 - \gamma_5}{2} \\
 &+ \{ [1 - 2n_f(\vec{p})] \frac{p_0 + |\vec{p}|}{2|\vec{p}|} (\gamma_0|\vec{p}| - \vec{\gamma}\vec{p})
 \end{aligned}$$

$$\begin{aligned}
& -[1 - 2n_f(-\vec{p})] \frac{p_0 - |\vec{p}|}{2|\vec{p}|} (\gamma_0 |\vec{p}| + \vec{\gamma} \vec{p}) \left\{ \frac{1 - \gamma_5}{2} \right\} * im_j(-i\cancel{p}) \\
& \times U_{\alpha,j}^* \frac{p^2 + m_j \cancel{p}}{(p^2 - m_j^2 - ip_0 \epsilon)(p^2 - ip_0 \epsilon)} U_{\beta,j}, \tag{20}
\end{aligned}$$

where f is the flavor of the initial neutrino beam.

The resummed Keldysh component $\tilde{S}_{\beta,\alpha,K}$ of the neutrino propagator consists of two contributions: (a) terms without $*$ -products (which we call algebraic) and (b) the terms with a single $*$ -product (which we call convolutional).

This propagator carries the information which, after the equal time limit, provides the number and momentum distribution of all types of flavor neutrinos measured at time t .

3.3. The $*$ -Products and the Average of Equal Time Limits

The remaining $*$ -product in (20) between the retarded and advanced functions is expressed (see Equation (A2) for details) as follows:

$$\begin{aligned}
C_{X_0}(p_0, \vec{p}) &= \int dp_{01} dp_{02} P_{X_0}(p_0, \frac{p_{01} + p_{02}}{2}) \frac{i}{2\pi} \frac{e^{-iX_0(p_{01} - p_{02} + i\epsilon)} - 1}{p_{01} - p_{02} + i\epsilon} A_{\infty,R}(p_{01}, \vec{p}) B_{\infty,A}(p_{02}, \vec{p}), \\
P_{X_0}(p_0, p'_0) &= \frac{1}{\pi} \Theta(X_0) \frac{\sin(2X_0(p_0 - p'_0))}{p_0 - p'_0}, \tag{21}
\end{aligned}$$

where the label ∞ means that the values of A and B should be taken at infinite time. After time t , the number of oscillating neutrinos is expressed through the average equal-time limit of the re-summed Keldysh component $\tilde{S}_{\beta,\alpha,K}$ of the neutrino propagator (see Appendix A):

$$\begin{aligned}
& 1 - \langle N_{\beta,\vec{p}}(t) \rangle \\
&= \frac{1}{2\pi} \left[\lim_{0 < \Delta \rightarrow 0} + \lim_{0 > \Delta \rightarrow 0} \right] \int dp_0 e^{-ip_0 \Delta} \text{Tr} \left[\frac{\gamma_0}{4} \tilde{S}_{\beta,\beta,K,t}(p) \frac{1 - \gamma_5}{2} \right], \tag{22}
\end{aligned}$$

where $\Delta = s_{01} - s_{02}$ and $X_0 = (s_{01} + s_{02})/2 = t$. In this expression, we have taken into account that the initial condition (A13) contains only flavor neutrinos of type f , not antineutrinos, and we calculate number of flavor neutrinos of type β . The equal time limit removes projector P from the above $*$ -product:

$$\frac{1}{\pi} \lim_{\Delta \rightarrow 0} \int dp_0 e^{-i\Delta p_0} C_{s_{02}=t}(p_0, \vec{p}) = \int dp_{01} dp_{02} \frac{i}{2\pi} \frac{e^{-it(p_{01} - p_{02})} - 1}{p_{01} - p_{02}} A_{\infty,R}(p_{01}, \vec{p}) B_{\infty,A}(p_{02}, \vec{p}). \tag{23}$$

3.4. Contributions to Neutrino Oscillation

To calculate neutrino oscillation, we start with chiral fermion number (22) and insert the solution of the Dyson–Schwinger Equation (20).

Upon managing all $*$ -products appearing in (20), we end up with two types of contributions:

1. Contributions without any $*$ -product. These contributions (the first pair in (20)) are independent in time. They should reproduce the initial (input) density of neutrinos. By calculating geometrical series term by term, one would obtain the lowest order providing the input neutrino density. All the higher term would vanish, as they are equal time limit of the product of two or more retarded functions (or two or more advanced functions). The re-summed propagator is nonperturbative, and consequently the result renormalizes the initial density. Nevertheless, we obtain the input neutrino density.

- Contributions containing $S_{\alpha,K}$ (the second pair in (20)). These refer to the initial input of flavor neutrinos of type α . They contribute to oscillation.

3.5. The Algebraic Term

Note here that we have to decide whether we approach equal time from above or from below. The final result does not depend on our choice; however, for our choice $\Delta = s_{01} - s_{02} > 0$ the advanced contribution should vanish.

We calculate the contribution of $[1 - iS_R\Sigma_R]^{-1}S_{\alpha,K,R}$ (at $n_f(-\vec{p}) = 0$)

$$\begin{aligned}
 I_{\alpha,alg} &= 1 - \langle N_{\alpha,alg}(\vec{p})(t) \rangle = \frac{i}{\pi} \lim_{s_{01} \rightarrow s_{02}=t} \int dp_0 e^{-ip_0(s_{01}-s_{02})} \\
 &\frac{1}{4} Tr \gamma_0 \delta_{\alpha,f} \sum_i U_{\alpha,i}^* U_{\alpha,i} \frac{i}{p^2 - m_i^2 + ip_0 \epsilon} [1 - 2n_f(\vec{p})] \frac{p_0 + |\vec{p}|}{2|\vec{p}|} (\gamma_0 |\vec{p}| - \vec{\gamma} \vec{p}) \frac{1 - \gamma_5}{2} \\
 &\frac{1}{4} Tr \gamma_0 (\theta + \eta \not{p}) (\gamma_0 |\vec{p}| + \vec{\gamma} \vec{p}) [1 - \gamma_5] = \theta |\vec{p}| \\
 I_{\alpha,alg} &= \lim_{s_{01} \rightarrow s_{02}=t} \int dp_0 e^{-ip_0(s_{01}-s_{02})} \sum_i |U_{\alpha,i}|^2 \frac{i}{p^2 - m_i^2 + ip_0 \epsilon} [1 - 2n_f(\vec{p})] \frac{p_0 + |\vec{p}|}{2\pi} \tag{24}
 \end{aligned}$$

Finally, we find

$$I_{\alpha,alg} = \delta_{\alpha,f} [1 - n_f(\vec{p})]. \tag{25}$$

This contribution is the only time-independent contribution to neutrino yield. As we will see, it confirms the conservation of the total number of neutrinos in our model. It indicates that the eventual (finite) wave function renormalization is not necessary.

3.6. *-Product, Term Containing $S_{K,R}$

In the terms with a convolution product, the chirality projector ($\frac{1-\gamma_5}{2}$) appears twice: once to select chiral neutrinos in initial distribution function, and a second time to be selected by the weak interaction measurement device:

$$\begin{aligned}
 I_{S_{conv},S_{K,R}} &= \frac{1}{4} Tr \gamma_0 \frac{i}{2\pi^2} \int dp_{01} dp_{02} \frac{e^{-i(p_{01}-p_{02})t} - 1}{p_{01} - p_{02}} \\
 &i[1 - i\Sigma S_R]^{-1} S_{K,R} \{p_{01}\} \{\Sigma S_A [1 - i\Sigma S_A]^{-1}\} \{p_{02}\} [1 - \gamma_5] / 2 \\
 &= \delta_{\alpha,f} \sum_{i,j} U_{\beta,i}^* U_{\alpha,i} U_{\alpha,j}^* U_{\beta,j} Tr \gamma_0 \frac{i}{16\pi^2} \int dp_{01} dp_{02} \frac{e^{-i(p_{01}-p_{02})t} - 1}{p_{01} - p_{02}} i \frac{p_1^2 + m_i \not{p}_1}{(p_1^2 - m_i^2 + ip_{01} \epsilon)(p_1^2 + ip_{01} \epsilon)} \\
 &\{[1 - 2n_f(\vec{p})] \frac{p_{01} + |\vec{p}|}{2|\vec{p}|} (\gamma_0 |\vec{p}| - \vec{\gamma} \vec{p}) - [1 - 2n_f(-\vec{p})] \frac{p_{01} - |\vec{p}|}{2|\vec{p}|} (\gamma_0 |\vec{p}| + \vec{\gamma} \vec{p})\} [1 - \gamma_5] m_j (-i\not{p}_2) \\
 &\times \frac{p_2^2 + m_j \not{p}_2}{(p_2^2 - m_j^2 - ip_{02} \epsilon)(p_2^2 - ip_{02} \epsilon)} \frac{1 - \gamma_5}{2} \\
 p_1 &= (p_{01}, \vec{p}), \quad p_2 = (p_{02}, \vec{p}). \tag{26}
 \end{aligned}$$

The trace is

$$\frac{1}{4} Tr \gamma_0 (p_1^2 + m_i \not{p}_1) [\gamma_0 |\vec{p}| \mp \vec{\gamma} \vec{p}] [1 - \gamma_5] (m_j + \not{p}_2) [1 - \gamma_5] = 2m_j p_1^2 |\vec{p}|. \tag{27}$$

Now, we have

$$I_{S_{conv,S_{K,R}}} = i\delta_{\alpha,f} \sum_{ij} U_{\beta,i}^* U_{\alpha,i} U_{\alpha,j}^* U_{\beta,j} \frac{im_j^2}{4\pi^2} \int dp_{01} dp_{02} \frac{e^{-i(p_{01}-p_{02})t} - 1}{p_{01} - p_{02}} \frac{\{[1 - 2n_f(\vec{p})](p_{01} + |\vec{p}|) - [1 - 2n_f(-\vec{p})](p_{01} - |\vec{p}|)\}}{(p_1^2 - m_i^2 + ip_{01}\epsilon)(p_2^2 - m_j^2 - ip_{02}\epsilon)}. \tag{28}$$

The integrals are performed by closing the integration path from below for dp_{01} and from above for dp_{02} .

$$\int dp_{01} \frac{e^{-i(p_{01}-p_{02})t} - 1}{p_{01} - p_{02}} \frac{p_{01} \pm |\vec{p}|}{p_1^2 - m_i^2 + i\epsilon p_{01}} = -i\pi \sum_{\lambda_i=\pm 1} \frac{(e^{-i(\lambda_i\omega_i-p_{02})t} - 1)(\omega_i \pm \lambda_i|\vec{p}|)}{\omega_i(\lambda_i\omega_i - p_{02})}$$

$$\int dp_{02} \frac{e^{-i(\lambda_i\omega_i-p_{02})t} - 1}{(\lambda_i\omega_i - p_{02})(p_2^2 - m_j^2 - ip_{02}\epsilon)} = i\pi \sum_{\lambda_j=\pm 1} \lambda_j \frac{e^{-i(\lambda_i\omega_i-\lambda_j\omega_j)t} - 1}{\omega_j(\lambda_i\omega_i - \lambda_j\omega_j)} \tag{29}$$

Here, $\omega_i = [|\vec{p}|^2 + m_i^2]^{1/2}$ and $\omega_j = [|\vec{p}|^2 + m_j^2]^{1/2}$

Thus, the contribution consists of contributions from all singularities (four terms):

$$I_{S_{conv,S_{K,R}}} = -\frac{m_j^2}{4} \delta_{\alpha,f} \sum_{ij} U_{\beta,i}^* U_{\alpha,i} U_{\alpha,j}^* U_{\beta,j} \sum_{\lambda_i,\lambda_j=\pm 1} \lambda_j \frac{e^{-i(\lambda_i\omega_i-\lambda_j\omega_j)t} - 1}{\omega_i\omega_j(\lambda_i\omega_i - \lambda_j\omega_j)} [\lambda_i|\vec{p}| - n_f(\vec{p})(\omega_i + \lambda_i|\vec{p}|) + n_f(-\vec{p})(\omega_i - \lambda_i|\vec{p}|)]. \tag{30}$$

After setting $n_{-\alpha}(-\vec{p}) = 0$, the integral is

$$I_{S_{conv,S_{K,R}}} = -\frac{m_j^2}{4} \delta_{\alpha,f} \sum_{ij} U_{\beta,i}^* U_{\alpha,i} U_{\alpha,j}^* U_{\beta,j} \sum_{\lambda_i,\lambda_j=\pm 1} \lambda_j \frac{e^{-i(\lambda_i\omega_i-\lambda_j\omega_j)t} - 1}{\omega_i\omega_j(\lambda_i\omega_i - \lambda_j\omega_j)} [\lambda_i|\vec{p}| - n_f(\vec{p})(\omega_i + \lambda_i|\vec{p}|)]$$

$$\omega_i = [|\vec{p}|^2 + m_i^2]^{1/2}, \quad \omega_j = [|\vec{p}|^2 + m_j^2]^{1/2}. \tag{31}$$

3.7. *-Product, Term Containing $S_{K,A}$ and $i \leftrightarrow j$ Terms

This integral is similar to the previous one:

$$I_{S_{conv,S_{K,A}}} = -\frac{m_i^2}{4} \delta_{\alpha,f} \sum_{ij} U_{\beta,i}^* U_{\alpha,i} U_{\alpha,j}^* U_{\beta,j} \sum_{\lambda_i,\lambda_j=\pm 1} \lambda_i \frac{e^{-i(\lambda_i\omega_i-\lambda_j\omega_j)t} - 1}{\omega_i\omega_j(\lambda_i\omega_i - \lambda_j\omega_j)} [\lambda_j|\vec{p}| - n_f(\vec{p})(\omega_j + \lambda_j|\vec{p}|)]. \tag{32}$$

With i and j interchanged, the contributions are

$$I_{S_{conv,S_{K,R}ji}} = -\frac{m_i^2}{4} \delta_{\alpha,f} \sum_{ij} U_{\beta,j}^* U_{\alpha,j} U_{\alpha,i}^* U_{\beta,i} \sum_{\lambda_i,\lambda_j=\pm 1} \lambda_i \frac{e^{-i(\lambda_j\omega_j-\lambda_i\omega_i)t} - 1}{\omega_i\omega_j(\lambda_j\omega_j - \lambda_i\omega_i)} [\lambda_j|\vec{p}| - n_f(\vec{p})(\omega_{ki} + \lambda_i|\vec{p}|)] \tag{33}$$

and

$$I_{S_{conv,S_{K,A}ji}} = -\frac{m_j^2}{4} \delta_{\alpha,f} \sum_{ij} U_{\beta,j}^* U_{\alpha,j} U_{\alpha,i}^* U_{\beta,i} \sum_{\lambda_i,\lambda_j=\pm 1} \lambda_j \frac{e^{-i(\lambda_j\omega_j-\lambda_i\omega_i)t} - 1}{\omega_i\omega_j(\lambda_j\omega_j - \lambda_i\omega_i)}$$

$$[\lambda_i |\vec{p}| - n_f(\vec{p})(\omega_{ki} + \lambda_i |\vec{p}|)]. \quad (34)$$

3.8. The Dominant Contribution

The results of the previous section are consistent with Heisenberg's uncertainty condition between energy and time. In our further calculations, we assume that the time is large compared to the energy differences $|\omega_i - \omega_j|$. Together with the fact that the measured neutrinos ($m_i \ll |\vec{p}|$) are mostly ultrarelativistic, with $|\vec{p}|$ ranging from 1 MeV to 10 MeV, the following approximations are justified:

$$\omega_i - \omega_j \approx \frac{m_i^2 - m_j^2}{2|\vec{p}|}, \quad \omega_i + \omega_j \approx 2|\vec{p}|, \quad \omega_i + |\vec{p}| \approx 2|\vec{p}| \quad \text{and} \quad \omega_i - |\vec{p}| \approx \frac{m_i^2}{2|\vec{p}|}. \quad (35)$$

Owing to the above, all contributions proportional to $[1 - 2n_f(\vec{p})]$ are dominated by $\lambda_i = \lambda_j = +1$, while the contributions proportional to $[1 - 2n_{\alpha,-}(-\vec{p})]$ are dominated by $\lambda_i = \lambda_j = -1$. The contribution from the constant 1 in $[1 - 2n_f]$ is killed by this procedure.

Notice, however, that for short times ($t \leq \frac{\hbar}{4\pi|\omega_i - \omega_j|}$, $i \neq j$) the approximations are not justified, and it is necessary to deal with the full expression. In order to satisfy Heisenberg's uncertainty relations among time and energy.

The above contributions then become

$$I_{S_{conv}, S_{K,R}^d} = m_j^2 \delta_{\alpha,f} \sum_{ij} U_{\beta,i}^* U_{\alpha,i} U_{\alpha,j}^* U_{\beta,j} \frac{e^{-i \frac{m_i^2 - m_j^2}{2|\vec{p}|} t} - 1}{m_i^2 - m_j^2} n_f(\vec{p}) \quad (36)$$

$$I_{S_{conv}, S_{K,A}^d} = m_i^2 \delta_{\alpha,f} \sum_{ij} U_{\beta,i}^* U_{\alpha,i} U_{\alpha,j}^* U_{\beta,j} \frac{e^{-i \frac{m_i^2 - m_j^2}{2|\vec{p}|} t} - 1}{m_i^2 - m_j^2} n_f(\vec{p}) \quad (37)$$

$$I_{S_{conv}, S_{K,R}^{jid}} = m_i^2 \delta_{\alpha,f} \sum_{ij} U_{\beta,j}^* U_{\alpha,j} U_{\alpha,i}^* U_{\beta,i} \frac{e^{i \frac{m_i^2 - m_j^2}{2|\vec{p}|} t} - 1}{m_i^2 - m_j^2} n_f(\vec{p}) \quad (38)$$

and

$$I_{S_{conv}, S_{K,A}^{jid}} = m_j^2 \delta_{\alpha,f} \sum_{ij} U_{\beta,j}^* U_{\alpha,j} U_{\alpha,i}^* U_{\beta,i} \frac{e^{i \frac{m_i^2 - m_j^2}{2|\vec{p}|} t} - 1}{m_i^2 - m_j^2} n_f(\vec{p}). \quad (39)$$

By adding the contributions, we obtain

$$\begin{aligned} I_{S_{conv}, S_K} &= I_{S_{conv}, S_{K,R}^d} - I_{S_{conv}, S_{K,A}^d} + I_{S_{conv}, S_{K,R}^{jid}} - I_{S_{conv}, S_{K,A}^{jid}} \\ &= \delta_{\alpha,f} \sum_{i \leq j} \{ U_{\beta,i}^* U_{\alpha,i} U_{\alpha,j}^* U_{\beta,j} [e^{-i \frac{m_i^2 - m_j^2}{2|\vec{p}|} t} - 1] - [U_{\beta,j}^* U_{\alpha,j} U_{\alpha,i}^* U_{\beta,i} e^{i \frac{m_i^2 - m_j^2}{2|\vec{p}|} t} - 1] \} n_f(\vec{p}), \end{aligned} \quad (40)$$

which can be further written as

$$\begin{aligned} I_{S_{conv}, S_K} &= -n_f(\vec{p}) \sum_{i \leq j} \\ &\delta_{\alpha,f} n_f(\vec{p}) \left[-4 \operatorname{Re}(U_{\beta,i}^* U_{\alpha,i} U_{\alpha,j}^* U_{\beta,j}) \sin^2 \frac{m_i^2 - m_j^2}{4|\vec{p}|} t + 2 \operatorname{Im}(U_{\beta,j}^* U_{\alpha,j} U_{\alpha,i}^* U_{\beta,i}) \sin \frac{m_i^2 - m_j^2}{2|\vec{p}|} t \right]. \end{aligned} \quad (41)$$

4. Final Result

From the preceding section, notably Equation (22), and from Appendix A, notably Appendix A.8, it can be seen that at time t the total number of particles of the flavor β stemming from the initial flavor α is

$$\begin{aligned} \langle N_{\beta,f,\vec{p}}(t) \rangle = & \delta_{\alpha,f} n_{\alpha,+}(\vec{p}) + n_f(\vec{p}) \delta_{\alpha,f} \sum_{i \leq j} \left[-4 \operatorname{Re}(U_{\beta,i}^* U_{\alpha,i} U_{\alpha,j}^* U_{\beta,j}) \sin^2 \frac{m_{ki}^2 - m_{lj}^2}{4|\vec{p}|} t \right. \\ & \left. + 2 \operatorname{Im}(U_{\beta,j}^* U_{\alpha,j} U_{\alpha,i}^* U_{\beta,i}) \sin \frac{m_i^2 - m_j^2}{2|\vec{p}|} t \right]. \end{aligned} \quad (42)$$

Let us point out a few features of this expression:

1. The result (42) is identical to the standard PMNS expression (4). The ultrarelativistic relation (3) reveals the equality of the arguments of the sines, while division by the initial distribution of the number of particles n_f recasts (42) in terms of probability, as in (4). Thus, with the same presently available inputs, our result (42) would provide the same numerical results as, for example, [86].
2. If we sum over β , the oscillating contribution vanishes. This reflects the fact that the total neutrino number is conserved within the realm of chiral neutrinos; notably, the sterile neutrinos are not involved! Notice that our conclusion is valid for low energy neutrino beams as well; this is easily verified by looking at (31)–(34).
3. The results are valid for moderate energies, although it is necessary to skip the simplifications in (3) and (35) and include all contributions.

Conclusions

In this paper, we apply the Finite Time Path Field Theory (FTPFT), originally designed to deal with out-of-equilibrium many-body statistical ensembles, to the problem in particle physics. We demonstrate that FTPFT is an appropriate tool for the treatment of neutrino oscillations.

We calculate neutrino oscillation within a simple model, with the interaction Lagrangian containing the term \mathcal{L}_{Mix} built as mass mixing through the PMNS-matrix with a built-in Dirac spinor and chirality structure. The model is exactly solvable. This is an extension of standard PMNS-case, as it involves sterile neutrinos, at least those with the same mass as flavor and propagating neutrinos. Of course, more sophisticated sterile neutrinos would require additional model building.

The result is consistent with Heisenberg's uncertainty relation between energy and time. The flavor neutrinos are chiral spin 1/2 particles, though a massive neutrino propagator should additionally contain the right-handed component along with the re-summed oscillating propagator. Nevertheless, the result is chirally invariant, as it is dictated from the weak interaction Lagrangian (\mathcal{L}_W) taken into account through the factors $(1 - \gamma_5)$ appearing at the beginning (production) and end (detection) stages. The sterile neutrinos do not contribute to oscillations, even for low energy beams. Our result coincides with the PMNS-formula for large times and for the ultrarelativistic case.

In the derivation of our result, the PMNS relation (1) is not used. Instead of using the relation which mixes flavor and propagating neutrino states (and in which at least one state cannot be on mass shell), the mass mixing Lagrangian through DSE provides an equally significant relation among the oscillating neutrino propagators obtained from DSE (18) and (19). They enable the calculation of the Keldysh component of the propagator $\tilde{S}_{\beta,\alpha,K}$ (20), which by application of AETL provides measurable particle numbers (42).

The FTPFT approach successfully passes the test of neutrino oscillations, in the sense that we demonstrate how to perform calculations of these oscillations using the presented approach. We reproduce the standard PMNS results in the present model, which introduces the neutrino masses precisely through the PMNS-matrix in the mixing part of the model Lagrangian. This means that while the present approach does not address the issue of the

origin of neutrino masses, and in general does not provide answers about the dynamics and physics of processes, the existing knowledge can be used as an input in the form of masses, matrices, self-energies, etc.

The application of the FTPFT approach to neutrino oscillations shows that it is an interesting candidate for a complementary tool to the S-matrix, which is formulated for infinite times and involves switching interactions on and off adiabatically. In the case of phenomena where finite times are essential, such as the presently pertinent neutrino oscillations as well as the oscillation of kaons and B and D mesons, decays, and symmetry violations, it has been necessary to use largely heuristic methods, such as elementary quantum mechanics in the PMNS approach and the Gell-Mann–Pais approach for kaons. In such cases, the FTPFT approach is obviously a candidate for a more rigorous description.

Further tests of the FTPFT approach could proceed along the following main lines:

1. Improving the model by taking into account the eventually-confirmed anomalies.
2. If suitable for considering decays of heavier neutrinos, the model could be easily adapted to build these features in. In this case, the self-energies should again be provided through an adequate calculation.
3. Applying the formalism to other oscillating and decay processes (e.g., decays of K^0 , D^0 , and B^0 mesons, positronium, the Cabibbo angle, etc.). This work is in progress and almost completed. It roughly confirms the Gell-Mann–Pais results. The factor which limits the predictive power is the rudimentary knowledge of the self-energies in the existing literature. Authors have mostly been concerned with obtaining the imaginary parts (decay rates), while the real parts (mass shifts) often involve renormalization.
4. In a classical out-of-equilibrium problem, the damping rates are the first thing to address. Braaten–Pisarski re-summation has provided a good start. Even for this case, two-loop self-energy diagrams contain minimal time vertices, and possible “upgrades” could be very tricky. This is another area where work is in progress.

Author Contributions: Conceptualization, I.D. and D.K.; Methodology, I.D.; Software, I.D.; Validation, I.D. and D.K.; Formal analysis, D.K.; Investigation, D.K.; Data curation, D.K.; Writing—original draft, D.K. All authors have read and agreed to the published version of the manuscript.

Funding: This research received no external funding.

Data Availability Statement: No new data were created in this study.

Conflicts of Interest: The authors declare no conflict of interest.

Appendix A

Appendix A.1. Finite Time Path Field Theory

To calculate neutrino oscillations, we use Finite Time Path Field Theory (FTPFT), often called the closed time path thermal field theory (CTP-TFT). “Thermal” is used here for historical reasons, as the theory was first constructed to treat ensembles at the thermal equilibrium or very close to it. Now, we find it to be an appropriate tool for calculation of a wide variety of problems, including equilibrium and nonequilibrium TFT problems (within the linear response approximation) as well as scattering processes, decays, and oscillations. There are a number of specific features distinguishing it from S-matrix theory:

1. The time path C is closed and finite: $C = (0 + i\epsilon, t + i\epsilon)U(t + i\epsilon, t - i\epsilon)U(t - i\epsilon, 0 - i\epsilon)$.
2. The subject of the S-matrix is amplitude (“wave function”), while in FTPFT it is a two-point function.
3. The product of two point functions is not algebraic, instead being a convolution product (see Appendix A.2); only under special conditions does it become an algebraic product.
4. Instead of Feynman propagators, matrix propagators S_{ij} , $i = 1, 2$, $j = 1, 2$ are obtained. These are linearly transformed into S_R (retarded), S_A (advanced), and S_K (Keldysh) propagators. Our method further separates S_K into its retarded and ad-

- vanced pieces ($S_K = S_{K,R} - S_{K,A}$); S_K contains single particle distribution functions of the unperturbed system (i.e., as they are determined at $t = 0$).
5. A measured quantity is obtained as an equal time limit of S_K . Compared to a scattering matrix, these measured quantities are more inclusive: one particle is separated (and measured), while the others are integrated over. This is equivalent to the exclusive S-matrix approach. In addition, the calculated quantities correspond to a yield, i.e., the number of particles found at time t , while the equivalent in the S-matrix approach is the cross-section, i.e., related to the time derivative of the yield.
 6. While primarily developed for thermal equilibrium and out-of-equilibrium (particularly "almost equilibrated") ensembles, nothing prevents it from being applied to decays and oscillations (as in this paper), or to scattering processes.
 7. For application to scattering processes, it is necessary to choose initial single particle distributions (i.e., for incoming particles) as two plane waves of extremely low intensities. After calculation it is then necessary to carry out the $t \rightarrow \infty$ limit. In our experience, the results are physically equivalent to S-matrix calculation. Adiabatic switching (on and off) of the interaction is not possible in finite time. With an infinite time limit ($t \rightarrow \infty$), the lack of adiabatic switching does not matter.

Appendix A.2. Convolution Product of Two Two-Point Functions

The convolution product [61] of two Green functions is defined as

$$C = A * B \Leftrightarrow C(x, y) = \int dz A(x, z) B(z, y). \quad (\text{A1})$$

In terms of Wigner transforms (see [61] for more details), it becomes

$$C_{X_0}(p_0, \vec{p}) = \int dp_{01} dp_{02} P_{X_0}(p_0, \frac{p_{01} + p_{02}}{2}) \frac{i}{2\pi} \frac{e^{-iX_0(p_{01} - p_{02} + i\epsilon)}}{p_{01} - p_{02} + i\epsilon} A_\infty(p_{01}, \vec{p}) B_\infty(p_{02}, \vec{p}), \quad (\text{A2})$$

where the projector P_{X_0} is

$$P_{X_0}(p_0, p'_0) = \frac{1}{2\pi} \Theta(X_0) \int_{-2X_0}^{2X_0} ds_0 e^{is_0(p_0 - p'_0)} = \frac{1}{\pi} \Theta(X_0) \frac{\sin(2X_0(p_0 - p'_0))}{p_0 - p'_0} \quad (\text{A3})$$

and

$$e^{-is_0 p'_0} \Theta(X_0) \Theta(2X_0 + s_0) \Theta(2X_0 - s_0) = \int dp_0 e^{-is_0 p_0} P_{X_0}(p_0, p'_0). \quad (\text{A4})$$

It is important to note that

$$\lim_{X_0 \rightarrow \infty} P_{X_0}(p_0, p'_0) = \lim_{X_0 \rightarrow \infty} \frac{1}{\pi} \frac{\sin(2X_0(p_0 - p'_0))}{p_0 - p'_0} = \delta(p_0 - p'_0). \quad (\text{A5})$$

The retarded (advanced) function is supposed to satisfy the following properties [61]:

- (1) The function of p_0 is analytic above (below) the real axis;
- (2) The function vanishes as $|p_0|$ approaches infinity in the upper (lower) semiplane.

If A is an advanced projected operator, we can integrate the expression (A2) even further. After closing the p_{01} integration contour in the lower semi-plane, we obtain

$$C_{X_0}(p_0, \vec{p}) = \int dp_{01} P_{X_0}(p_0, p_{01}) A_\infty(p_{01}, \vec{p}) B_\infty(p_{01}, \vec{p}). \quad (\text{A6})$$

If B is a retarded projected operator, we can achieve the same result by closing the p_{02} integration contour in the upper semi-plane.

In the $X_0 \rightarrow \infty$ limit (A5), Equation (A6) becomes the simple algebraic product

$$C_\infty(p_0, \vec{p}) = A_\infty(p_0, \vec{p}) B_\infty(p_0, \vec{p}). \quad (\text{A7})$$

Note that Equations (A6) and (A7) are valid for combinations $A_A B_A, A_A B_R, A_R B_R$, but not for $A_R B_A$.

For A_R (retarded) and B_A (advanced), the Equal Time Limit (ETL) of the convolution product is obtained as follows:

$$\frac{1}{\pi} \lim_{\Delta \rightarrow 0} \int dp_0 e^{-i\Delta p_0} C_{X_0}(p_0, \vec{p}) = \int dp_{01} dp_{02} \frac{i}{2\pi} \frac{e^{-iX_0(p_{01}-p_{02})} - 1}{p_{01} - p_{02}} A_{\infty,R}(p_{01}, \vec{p}) B_{\infty,A}(p_{02}, \vec{p}) \tag{A8}$$

where $\Delta = s_{01} - s_{02}$ and $X_0 = (s_{01} + s_{02})/2$. The ETL is finally changed to AETL (the average of ETL), where $\lim_{\Delta \rightarrow 0}$ is replaced by $\frac{1}{2}[\lim_{0 < \Delta \rightarrow 0} + \lim_{0 > \Delta \rightarrow 0}]$. From the numerator, the constant term (-1) could have been subtracted, because for this term it is possible to close the integration path dp_{01} from below (or to close the integration path dp_{02} from above), in order to find that the contribution vanishes. The resulting “kernel” is not singular, and we omit the $i\epsilon$ prescription.

From now on, we skip the index ∞ as self-understandable.

Appendix A.3. Massive Neutrino Propagator

The massive neutrino propagators with masses $m_i \neq 0, i = 1, 2, 3$ for the case when the fermion and antifermion distribution are equal:

$n_+(\omega_p, \vec{p}) = n_-(\omega_p, -\vec{p})$ is simple,

$$D_R(p) = (\not{p} + m) G_R(p, m),$$

$$D_A(p) = (\not{p} + m) G_A(p, m),$$

$$G_{R(A)}(p, m) = \frac{-i}{p^2 - m^2 \pm 2ip_0\epsilon},$$

$$D_K(p) = D_{K,R}(p) - D_{K,A}(p),$$

$$D_{K,R}(p) = -[1 - 2n(\omega_p)] (\not{P} + \frac{mp_0}{\omega_p}) G_R(p, m),$$

$$D_{K,A}(p) = -[1 - 2n(\omega_p)] (\not{P} + \frac{mp_0}{\omega_p}) G_A(p, m),$$

$$\not{p} = \gamma^\mu p_\mu, p = (p_0, \vec{p}), \not{P} = \gamma^\mu P_\mu, P = (\omega_p, \frac{p_0}{\omega_p} \vec{p}), \omega_p = \sqrt{\vec{p}^2 + m^2}, \tag{A9}$$

where $n(\omega_p)$ is the initial fermion distribution function.

Appendix A.4. “Flavor Neutrino” Propagator

Flavor neutrinos ν_e, ν_μ , and ν_τ are, by assumption, massless and chiral; only left-handed flavor neutrinos and right-handed antineutrinos exist:

$$S_{f,R}(p) = \not{p} G_R(p, 0),$$

$$S_{f,A}(p) = \not{p} G_A(p, 0),$$

$$G_{R(A)}(p, 0) = \frac{-i}{p^2 \pm 2ip_0\epsilon},$$

$$\not{p} = \gamma^\mu p_\mu, p = (p_0, \vec{p}), \not{P} = \gamma^\mu P_\mu, P = (|\vec{p}|, \frac{p_0}{|\vec{p}|} \vec{p}). \tag{A10}$$

For unequal flavor neutrino and flavor antineutrino distributions, we have

$$n(p_0, \vec{p}) = \frac{1 - \gamma_5}{2} \Theta(p_0) n_+(\vec{p}) - \frac{1 - \gamma_5}{2} \Theta(-p_0) n_-(-\vec{p}), \tag{A11}$$

where $n(p_0, \vec{p})$ is now a 4×4 matrix.

Now, we decompose Keldysh propagator into its retarded and advanced parts:

$$\begin{aligned} S_{f,K}(p) &= S_{f,K,R}(p) - S_{f,K,A}(p), \\ S_{f,K,R}(p) &= -G_R(p, 0) L_f(p_0, \vec{p}), \\ S_{f,K,A}(p) &= -G_A(p, 0) L_f(p_0, \vec{p}), \end{aligned} \tag{A12}$$

where

$$\begin{aligned} L_f(p_0, \vec{p}) &= [1 - 2n_f(\vec{p})] \frac{p_0 + |\vec{p}|}{2|\vec{p}|} (\gamma_0 |\vec{p}| - \vec{\gamma} \vec{p}) \frac{1 - \gamma_5}{2} \\ &- [1 - 2n_{\bar{f}}(-\vec{p})] \frac{p_0 - |\vec{p}|}{2|\vec{p}|} (\gamma_0 |\vec{p}| + \vec{\gamma} \vec{p}) \frac{1 - \gamma_5}{2}. \end{aligned} \tag{A13}$$

We define the propagator for flavor antineutrinos by \bar{S} , which is obtained from S via the replacement of $n_f \leftrightarrow n_{\bar{f}}$. These propagators satisfy the following properties under inversion:

$$S_{f,R}(-p) = -\bar{S}_{f,A}(p), \quad S_{f,K,R}(-p) = -\bar{S}_{f,K,A}(p).$$

Appendix A.5. Oscillating Neutrino Propagator

In addition to flavor and propagating neutrinos, we have defined “oscillating neutrinos” above by solving Equations (12)–(15) through partial re-summation of DSE over the powers of the mixing mass interaction self-energies.

Appendix A.6. Dyson–Schwinger Equation for Fermions

Here, S is the lowest order Green function and \tilde{S} is the re-summed Green function:

$$[S^{-1} - i\Sigma] * \tilde{S} = 1, \tag{A14}$$

where

$$\begin{aligned} S &= \begin{pmatrix} S_R & S_K \\ 0 & S_A \end{pmatrix}, \quad \Sigma = \begin{pmatrix} \Sigma_R & \Sigma_K \\ 0 & \Sigma_A \end{pmatrix}, \\ \tilde{S} &= \begin{pmatrix} \tilde{S}_R & \tilde{S}_K \\ 0 & \tilde{S}_A \end{pmatrix} \end{aligned} \tag{A15}$$

or in components,

$$\begin{aligned} \tilde{S}_R &= S_R + iS_R * \Sigma_R * \tilde{S}_R \\ \tilde{S}_A &= S_A + iS_A * \Sigma_A * \tilde{S}_A \\ \tilde{S}_K &= S_K + i[S_R * \Sigma_K * \tilde{S}_A \\ &+ S_K * \Sigma_A * \tilde{S}_A + S_R * \Sigma_R * \tilde{S}_K]. \end{aligned} \tag{A16}$$

The formal solution is

$$\begin{aligned}\tilde{S}_R &= [1 - iS_R * \Sigma_R]^{-1} * S_R = S_R * [1 - i\Sigma_R * S_R]^{-1}, \\ \tilde{S}_A &= [1 - iS_A * \Sigma_A]^{-1} * S_A = S_A * [1 - i\Sigma_A * S_A]^{-1}, \\ \tilde{S}_K &= +i\tilde{S}_R \Sigma_K \tilde{S}_A + \tilde{S}_R S_R^{-1} S_K S_A^{-1} \tilde{S}_A\end{aligned}\quad (\text{A17})$$

$$\begin{aligned}\tilde{S}_K &= -S_{K,A} * (1 - i\Sigma_A * S_A)^{-1} + (1 - iS_R * \Sigma_R)^{-1} * S_{K,R} \\ &+ i(1 - iS_R * \Sigma_R)^{-1} * [S_R * \Sigma_K * S_A - S_R * \Sigma_R * S_{K,A} \\ &+ S_{K,R} * \Sigma_A * S_A] * (1 - i\Sigma_A * S_A)^{-1},\end{aligned}\quad (\text{A18})$$

where we have used

$$S_K = S_{K,R} - S_{K,A}, \quad \Sigma_K = \Sigma_{K,R} - \Sigma_{K,A}.\quad (\text{A19})$$

Appendix A.7. Fermion Particle Number

The number of fermions of momentum \vec{p} at the time t is obtained from the time evolution of the of number operator, which is the Average of the Equal Time Limit (AETL) of the propagator $S_{K,s_{01},s_{02}}$. The average is necessary because we must distinguish the limit from above $s_{01} - s_{02} = \Delta > 0$ and the limit from below $\Delta < 0$. If the propagator $\tilde{S}_{K,s_{01},s_{02}}(p)$ has a pole which is apart from the real axis for the finite imaginary part, these two limits will be different, in which case we take the average. Using AETL, we are able to understand the limit:

$$\text{AETL} = \frac{1}{2} \left[\lim_{0 < \Delta \rightarrow 0} + \lim_{0 > \Delta \rightarrow 0} \right].\quad (\text{A20})$$

The particle number is defined as

$$\langle N_{\vec{p}}(t) \rangle = (2\pi)^3 d\mathcal{N} / (d^3x d^3p)\quad (\text{A21})$$

and

$$1 - \langle N_{f,\vec{p}}(t) \rangle = \frac{1}{2\pi} \left[\lim_{0 < \Delta \rightarrow 0} + \lim_{0 > \Delta \rightarrow 0} \right] \int dp_0 e^{-ip_0 \Delta} \text{Tr} \left[\frac{\gamma_0}{4} \tilde{S}_{K,t}(p) \right],\quad (\text{A22})$$

where $\Delta = s_{01} - s_{02}$ and $X_0 = (s_{01} + s_{02})/2 = t$.

The contribution (A22) corresponds to a single polarization. To sum over the polarizations, an additional factor of 2 is necessary.

When acting on the momentum and spin eigenstates of fermions $|+, \vec{p}, s\rangle$ and antifermions $|-, -\vec{p}, s\rangle$ (both normalized to $\langle \pm, \pm \vec{p}, s | \pm, \pm \vec{p}, s \rangle = 1/m$), the projectors Λ_{\pm} satisfy

$$\begin{aligned}\Lambda_+(\omega_p, \vec{p})|+, \vec{p}, s\rangle &= |+, \vec{p}, s\rangle \quad \text{and} \quad \Lambda_-(\omega_p, \vec{p})|+, \vec{p}, s\rangle = 0, \quad \text{while} \\ \Lambda_+(\omega_p, \vec{p})|-, -\vec{p}, s\rangle &= 0 \quad \text{and} \quad \Lambda_-(\omega_p, \vec{p})|-, -\vec{p}, s\rangle = |-, -\vec{p}, s\rangle.\end{aligned}$$

In the rest of this paper, the distribution functions are assumed to depend on $|\vec{p}|$ and not on the direction of \vec{p} . The lowest order contribution ($N_{f+\vec{f},\vec{p}}^0(t)$) is identical to the initial distribution (for $n_{\vec{f}}(\omega_p) = 0$):

$$1 - \langle N_{f,\vec{p}}^0(t) \rangle = 1 - n_{+f}(\omega_p).\quad (\text{A23})$$

Appendix A.8. Massless Chiral Fermion Particle Number

For a massless *chiral* particle there is one more helicity projector $(1 - \gamma_5)/2$ with respect to the trace in Equation (A22). The particle number becomes (22):

$$1 - \langle N_{\beta, \vec{p}}(t) \rangle = \frac{1}{2\pi} \left[\lim_{0 < \Delta \rightarrow 0} + \lim_{0 > \Delta \rightarrow 0} \right] \int dp_0 e^{-ip_0 \Delta} \text{Tr} \left[\frac{\gamma_0}{4} \tilde{S}_{\beta, \beta, K, t}(p) \frac{1 - \gamma_5}{2} \right]. \quad (\text{A24})$$

Here, $\langle N_{\beta, \vec{p}}(t) \rangle$ is the number of neutrinos of flavor f and momentum \vec{p} detected at time t .

Note that one more helicity projector $\frac{1 - \gamma_5}{2}$ is necessary to ensure the proper helicity (chirality) of the detected neutrinos. The lowest-order contribution for a massless chiral particle is identical to the initial distribution:

$$1 - \langle N_{f \vec{p}}^0(t) \rangle = 1 - n_f(|\vec{p}|). \quad (\text{A25})$$

References

- Davis, R., Jr.; Harmer, D.S.; Hoffman, K.C. Search for neutrinos from the sun. *Phys. Rev. Lett.* **1968**, *20*, 1205–1209. [[CrossRef](#)]
- Fukuda, Y.; Hayakawa, T.; Ichihara, E.; Inoue, K.; Ishihara, K.; Ishino, H.; Itow, Y.; Kajita, T.; Kameda, J.; Kasuga, S.; et al. Evidence for oscillation of atmospheric neutrinos. *Phys. Rev. Lett.* **1998**, *81*, 1562. [[CrossRef](#)]
- Apollonio, M.; Baldini, A.; Bemporad, C.; Caffau, E.; Cei, F.; D’Eclaise, Y.; de Kerret, H.; Dieterle, B.; Etenko, A.; George, J.; et al. Limits on neutrino oscillations from the CHOOZ experiment. *Phys. Lett. B* **1999**, *466*, 415–430. [[CrossRef](#)]
- Abazajian, K.N.; Acero, M.A.; Agarwalla, S.K.; Aguilar-Arevalo, A.A.; Albright, C.H.; Antusch, S.; Argüelles, C.A.; Balantekin, A.B.; Barenboim, G.; Barger, V.; et al. Light Sterile Neutrinos: A White Paper. *arXiv* **2012**, arXiv:1204.5379.
- Aguilar, A.; Auerbach, L.B.; Burman, R.L.; Caldwell, D.O.; Church, E.D.; Cochran, E.D.; Donahue, J.B.; Fazely, A.; Garvey, G.T.; Gunasingha, R.M.; et al. Evidence for neutrino oscillations from the observation of $\bar{\nu}_e$ appearance in a $\bar{\nu}_\mu$ beam. *Phys. Rev. D* **2001**, *64*, 112007. [[CrossRef](#)]
- Schechter, J.; Valle, J.W.F. Neutrino Masses in SU(2) x U(1) Theories. *Phys. Rev. D* **1980**, *22*, 2227. [[CrossRef](#)]
- Eguchi, K.; Enomoto, S.; Furuno, K.; Goldman, J.; Hanada, H.; Ikeda, H.; Ikeda, K.; Inoue, K.; Ishihara, K.; Itoh, W.; et al. First results from KamLAND: Evidence for reactor anti-neutrino disappearance. *Phys. Rev. Lett.* **2003**, *90*, 021802. [[CrossRef](#)]
- Hosaka, J.; Ishihara, K.; Kameda, J.; Koshio, Y.; Minamino, A.; Mitsuda, C.; Miura, M.; Moriyama, S.; Nakahata, M.; Namba, T.; et al. Solar neutrino measurements in super-Kamiokande-I. *Phys. Rev. D* **2006**, *73*, 112001. [[CrossRef](#)]
- Cervera, A.; Donini, A.; Gavela, M.B.; Cadenas, J.J.G.; Hernandez, P.; Mena, O.; Rigolin, S. Golden measurements at a neutrino factory. *Nucl. Phys. B* **2001**, *579*, 17–55; Erratum in *Nucl. Phys. B* **2001**, *593*, 731–732. [[CrossRef](#)]
- Barger, V.; Marfatia, D.; Whisnant, K. Breaking eight fold degeneracies in neutrino CP violation, mixing, and mass hierarchy. *Phys. Rev. D* **2002**, *65*, 073023. [[CrossRef](#)]
- Yasuda, O. New plots and parameter degeneracies in neutrino oscillations. *New J. Phys.* **2004**, *6*, 83. [[CrossRef](#)]
- Burguet-Castell, J.; Gavela, M.B.; Gomez-Cadenas, J.J.; Hernandez, P.; Mena, O. On the Measurement of leptonic CP violation. *Nucl. Phys. B* **2001**, *608*, 301. [[CrossRef](#)]
- Minakata, H.; Nunokawa, H. Exploring neutrino mixing with low-energy superbeams. *J. High Energy Phys.* **2001**, 001. [[CrossRef](#)]
- Fogli, G.L.; Lisi, E. Tests of three flavor mixing in long baseline neutrino oscillation experiments. *Phys. Rev. D* **1996**, *54*, 3667. [[CrossRef](#)] [[PubMed](#)]
- Abe, K.; Abgrall, N.; Ajima, Y.; Aihara, H.; Albert, J.B.; Andreopoulos, C.; Andrieu, B.; Aoki, S.; Araoka, O.; Argyriades, J.; et al. Indication of Electron Neutrino Appearance from an Accelerator-produced Off-axis Muon Neutrino Beam. *Phys. Rev. Lett.* **2011**, *107*, 041801. [[CrossRef](#)] [[PubMed](#)]
- Adamson, P.; Auty, D.J.; Ayres, D.S.; Backhouse, C.; Barr, G.; Betancourt, M.; Bishai, M.; Blake, A.; Bock, G.J.; Boehnlein, D.J.; et al. Active to sterile neutrino mixing limits from neutral-current interactions in MINOS. *Phys. Rev. Lett.* **2011**, *107*, 181802. [[CrossRef](#)] [[PubMed](#)]
- Abe, Y.; Aberle, C.; Akiri, T.; dos Anjos, J.C.; Ardellier, A.F.; Barbosa, F.; Baxter, A.; Bergevin, M.; Bernstein, A.; Bezerra, T.J.C.; et al. Indication of Reactor $\bar{\nu}_e$ Disappearance in the Double Chooz Experiment. *Phys. Rev. Lett.* **2012**, *108*, 131801. [[CrossRef](#)]
- An, F.P.; Bai, J.Z.; Balantekin, A.B.; Band, H.R.; Beavis, D.; Beriguete, W.; Bishai, M.; Blyth, S.; Boddy, K.; Brown, R.L.; et al. Observation of electron-antineutrino disappearance at Daya Bay. *Phys. Rev. Lett.* **2012**, *108*, 171803. [[CrossRef](#)]
- Ahn, J.K.; Chebotaryov, S.; Choi, J.H.; Choi, S.; Choi, W.; Choi, Y.; Jang, H.I.; Jang, J.S.; Jeon, E.J.; Jeong, I.S.; et al. Observation of Reactor Electron Antineutrino Disappearance in the RENO Experiment. *Phys. Rev. Lett.* **2012**, *108*, 191802. [[CrossRef](#)]
- Abe, K.; Akhlaq, N.; Akutsu, R.; Ali, A.; Alt, C.; Andreopoulos, C.; Antonova, M.; Aoki, S.; Arihara, T.; Asada, Y.; et al. Neutron-antineutron oscillation search using a 0.37 megaton-years exposure of Super-Kamiokande. *Phys. Rev. D* **2021**, *103*, 112008. [[CrossRef](#)]

21. Acero, M.A.; Adamson, P.; Aliaga, L.; Anfimov, N.; Antoshkin, A.; Arrieta-Diaz, E.; Asquith, L.; Aurisano, A.; Back, A.; Backhouse, C.; et al Improved measurement of neutrino oscillation parameters by the NOvA experiment. *Phys. Rev. D* **2022**, *106*, 032004. [[CrossRef](#)]
22. Gonzalez-Garcia, M.C.; Maltoni, M.; Schwetz, T. NuFIT: Three-Flavour Global Analyses of Neutrino Oscillation Experiments. *Universe* **2021**, *7*, 459. [[CrossRef](#)]
23. Capozzi, F.; Valentino, E.D.; Lisi, E.; Marrone, A.; Melchiorri, A.; Palazzo, A. Unfinished fabric of the three neutrino paradigm. *Phys. Rev. D* **2021**, *104*, 083031. [[CrossRef](#)]
24. de Salas, P.F.; Forero, D.V.; Gariazzo, S.; Martínez-Miravé, P.; Mena, O.; Ternes, C.A.; Tórtola, M.; Valle, J.W.F. 2020 global reassessment of the neutrino oscillation picture. *J. High Energy Phys.* **2021**, *2*, 71. [[CrossRef](#)]
25. Cleveland, B.T.; Daily, T.; Davis, R., Jr.; Distel, J.R.; Lande, K.; Lee, C.K.; Wildenhain, P.S.; Ullman, J. Measurement of the solar electron neutrino flux with the Homestake chlorine detector. *Astrophys. J.* **1998**, *496*, 505–526. [[CrossRef](#)]
26. Kaether, F.; Hampel, W.; Heusser, G.; Kiko, J.; Kirsten, T. Reanalysis of the GALLEX solar neutrino flux and source experiments. *Phys. Lett. B* **2010**, *685*, 47–54. [[CrossRef](#)]
27. Abdurashitov, J.N.; Gavrin, V.N.; Gorbachev, V.V.; Gurkina, P.P.; Ibragimova, T.V.; Kalikhov, A.V.; Khairmasov, N.G.; Knodel, T.V.; Mirmov, I.N.; Shikhin, A.A.; et al. Measurement of the solar neutrino capture rate with gallium metal. III: Results for the 2002–2007 data-taking period. *Phys. Rev. C* **2009**, *80*, 015807. [[CrossRef](#)]
28. Cravens, J.P.; Abe, K.; Iida, T.; Ishihara, K.; Kameda, J.; Koshio, Y.; Minamino, A.; Mitsuda, C.; Miura, M.; Moriyama, S.; et al. Solar neutrino measurements in Super-Kamiokande-II. *Phys. Rev. D* **2008**, *78*, 032002. [[CrossRef](#)]
29. Abe, K.; Hayato, Y.; Iida, T.; Ikeda, M.; Ishihara, C.; Iyogi, K.; Kameda, J.; Kobayashi, K.; Koshio, Y.; Kozuma, Y.; et al. Solar neutrino results in Super-Kamiokande-III. *Phys. Rev. D* **2011**, *83*, 052010. [[CrossRef](#)]
30. Nakajima, Y. Recent results and future prospects from Super-Kamiokande. In Proceedings of the XXIX International Conference on Neutrino Physics and Astrophysics, Chicago, IL, USA, 22 June–2 July 2020. [[CrossRef](#)]
31. Aharmim, B.; Ahmed, S.N.; Anthony, A.E.; Barros, N.; Beier, E.W.; Bellerive, A.; Beltran, B.; Bergevin, M.; Biller, S.D.; Boudjemline, K.; et al. Combined Analysis of all Three Phases of Solar Neutrino Data from the Sudbury Neutrino Observatory. *Phys. Rev. C* **2013**, *88*, 025501. [[CrossRef](#)]
32. Bellini, G.; Benziger, J.; Bick, D.; Bonetti, S.; Bonfini, G.; Avanzini, M.B.; Caccianiga, B.; Cadonati, L.; Calaprice, F.; Carraro, C.; et al. Precision measurement of the ^7Be solar neutrino interaction rate in Borexino. *Phys. Rev. Lett.* **2011**, *107*, 141302. [[CrossRef](#)] [[PubMed](#)]
33. Bellini, G.; Benziger, J.; Bonetti, S.; Buizza Avanzini, M.; Caccianiga, B.; Cadonati, L.; Calaprice, F.; Carraro, C.; Chavarria, A.; Chepurnov, A.; et al. Measurement of the solar ^8B neutrino rate with a liquid scintillator target and 3 MeV energy threshold in the Borexino detector. *Phys. Rev. D* **2010**, *82*, 033006. [[CrossRef](#)]
34. Borexino Collaboration; Bellini, G.; Benziger, J.; Bick, D.; Bonfini, G.; Bravo, D.; Caccianiga, B.; Cadonati, L.; Calaprice, F.; Caminata, A.; et al. Neutrinos from the primary proton–proton fusion process in the Sun. *Nature* **2014**, *512*, 383–386.
35. Gando, A.; Gando, Y.; Hanakago, H.; Ikeda, H.; Inoue, K.; Ishidoshiro, K.; Ishikawa, H.; Koga, M.; Matsuda, R.; Matsuda, S.; et al. Reactor On-Off Antineutrino Measurement with KamLAND. *Phys. Rev. D* **2013**, *88*, 033001. [[CrossRef](#)]
36. Abe, K.; Bronner, C.; Haga, Y.; Hayato, Y.; Ikeda, M.; Iyogi, K.; Kameda, J.; Kato, Y.; Kishimoto, Y.; Marti, L.; et al. Atmospheric neutrino oscillation analysis with external constraints in Super-Kamiokande I-IV. *Phys. Rev. D* **2018**, *97*, 072001. [[CrossRef](#)]
37. Aartsen, M.G.; Ackermann, M.; Adams, J.; Aguilar, J.A.; Ahlers, M.; Ahrens, M.; Altmann, D.; Anderson, T.; Argüelles, C.; Arlen, T.C.; et al. Measurement of the Atmospheric ν_e Spectrum with IceCube. *Phys. Rev. D* **2015**, *91*, 072004. [[CrossRef](#)]
38. Bezerra, T. New Results from the Double Chooz Experiment. In Proceedings of the XXIX International Conference on Neutrino Physics and Astrophysics, Chicago, IL, USA, 22 June–2 July 2020. [[CrossRef](#)]
39. Adey, D.; An, F.P.; Balantekin, A.B.; Band, H.R.; Bishai, M.; Blyth, S.; Cao, D.; Cao, G.F.; Cao, J.; Chan, Y.L. Measurement of the Electron Antineutrino Oscillation with 1958 Days of Operation at Daya Bay. *Phys. Rev. Lett.* **2018**, *121*, 241805. [[CrossRef](#)]
40. Yoo, J. Recent Results from RENO Experiment. In Proceedings of the XXIX International Conference on Neutrino Physics and Astrophysics, Chicago, IL, USA, 22 June–2 July 2020. [[CrossRef](#)]
41. Adamson, P.; Anghel, I.; Backhouse, C.; Barr, G.; Bishai, M.; Blake, A.; Bock, G.J.; Bogert, D.; Cao, S.V.; Castromonte, C.M. Measurement of neutrino and antineutrino oscillations using beam and atmospheric data in MINOS. *Phys. Rev. Lett.* **2013**, *110*, 251801. [[CrossRef](#)]
42. Dunne, P. Latest Neutrino Oscillation Results from T2K. In Proceedings of the XXIX International Conference on Neutrino Physics and Astrophysics, Chicago, IL, USA, 22 June–2 July 2020. [[CrossRef](#)]
43. Himmel, A. New Oscillation Results from the NOvA Experiment. In Proceedings of the XXIX International Conference on Neutrino Physics and Astrophysics, Chicago, IL, USA, 22 June–2 July 2020. [[CrossRef](#)]
44. Altherr, T.; Salati, P. The Electric charge of neutrinos and plasmon decay. *Nucl. Phys. B* **1994**, *421*, 662–682. [[CrossRef](#)]
45. Ho, C.M.; Boyanovsky, D.; de Vega, H.J. Neutrino oscillations in the early universe: A Real time formulation. *Phys. Rev. D* **2005**, *72*, 085016. [[CrossRef](#)]
46. Blasone, M.; Jizba, P.; Mavromatos, N.E.; Smaldone, L. Dynamical generation of field mixing via flavor vacuum condensate. *Phys. Rev. D* **2019**, *100*, 045027. [[CrossRef](#)]
47. Blasone, M.; Smaldone, L.; Vitiello, G. Neutrino mixing, entanglement and the gauge paradigm in quantum field theory. *PoS CORFU2021* **2022**, 049. [[CrossRef](#)]

48. Blasone, M.; Smaldone, L.; Vitiello, G. Non-Abelian gauge structure and flavor mixing in quantum field theory. *J. Phys. Conf. Ser.* **2023**, *2533*, 012010. [[CrossRef](#)]
49. Schwinger, J. Brownian motion of a quantum oscillator. *J. Math. Phys.* **1961**, *2*, 407. [[CrossRef](#)]
50. Keldysh, L.V. Diagram technique for nonequilibrium processes. *Sov. Phys. JETP* **1965**, *20*, 1018–1026.
51. Kadanoff, L.P.; Baym, G. *Quantum Statistical Mechanics*; Benjamin: New York, NY, USA, 1962.
52. Danielewicz, P. Quantum Theory of Nonequilibrium Processes. 1. *Ann. Phys.* **1984**, *152*, 239. [[CrossRef](#)]
53. Chou, K.-C.; Su, Z.-B.; Hao, B.-L.; Yu, L. Equilibrium and Nonequilibrium Formalisms Made Unified. *Phys. Rep.* **1985**, *118*, 1. [[CrossRef](#)]
54. Rammer, J.; Smith, H. Quantum field-theoretical methods in transport theory of metals. *Rev. Mod. Phys.* **1986**, *58*, 323. [[CrossRef](#)]
55. Landsman, N.P.; van Weert, C.G. Real and Imaginary Time Field Theory at Finite Temperature and Density. *Phys. Rep.* **1987**, *145*, 141. [[CrossRef](#)]
56. Calzetta, E.; Hu, B.L. Nonequilibrium Quantum Fields: Closed Time Path Effective Action, Wigner Function and Boltzmann Equation. *Phys. Rev. D* **1988**, *37*, 2878. [[CrossRef](#)]
57. Bellac, M.L. *Thermal Field Theory*; Cambridge University Press: Cambridge, UK, 1996.
58. Brown, D.A.; Danielewicz, P. Partons in phase space. *Phys. Rev. D* **1998**, *58*, 094003. [[CrossRef](#)]
59. Dadić, I. Two mechanisms for elimination of pinch singularities in/out of equilibrium thermal field theories. *Phys. Rev. D* **1999**, *59*, 125012. [[CrossRef](#)]
60. Blaizot, J.-P.; Iancu, E. The Quark gluon plasma: Collective dynamics and hard thermal loops. *Phys. Rep.* **2002**, *359*, 355–528. [[CrossRef](#)]
61. Dadić, I. Out of equilibrium thermal field theories: Finite time after switching on the interaction and Wigner transforms of projected functions. *Phys. Rev. D* **2000**, *63*, 025011. [[CrossRef](#)]
62. Dadić, I. Out-of-equilibrium TFT-energy nonconservation at vertices. *Nucl. Phys. A* **2002**, *702*, 356. [[CrossRef](#)]
63. Arleo, F.; Aurenche, P.; Bopp, F.W.; Dadić, I.; David, G.; Delagrangé, H.; d’Enterria, D.G.; Eskola, K.J.; Gelis, F.; Guillet, J.P. Hard probes in heavy-ion collisions at the LHC: Photon physics in heavy ion collisions at the LHC. CERN Yellow Book CERN-2004-009-D. *arXiv* **2004**, arXiv:hep-ph/0311131.
64. Dadić, I. Retarded propagator representation of out-of-equilibrium thermal field theories. *Nucl. Phys. A* **2009**, *820*, 267C. [[CrossRef](#)]
65. Millington, P.; Pilaftsis, A. Perturbative nonequilibrium thermal field theory. *Phys. Rev. D* **2013**, *88*, 085009. [[CrossRef](#)]
66. Millington, P.; Pilaftsis, A. Thermal field theory to all orders in gradient expansion. *J. Phys. Conf. Ser.* **2013**, *447*, 012071. [[CrossRef](#)]
67. Dadić, I.; Klabučar, D. Causality and Renormalization in Finite-Time-Path Out-of-Equilibrium ϕ^3 QFT. *Particles* **2019**, *2*, 92–102. [[CrossRef](#)]
68. Dadić, I.; Klabučar, D.; Kuić, D. Direct photons from Quark Matter in Renormalized Finite-Time-Path QED. *Particles* **2020**, *3*, 676–692. [[CrossRef](#)]
69. Beuthe, M. Oscillations of neutrinos and mesons in quantum field theory. *Phys. Rept.* **2003**, *375*, 105–218. [[CrossRef](#)]
70. Akhmedov, E.K.; Kopp, J. Neutrino Oscillations: Quantum Mechanics vs. Quantum Field Theory. *J. High Energy Phys.* **2013**, *4*, 8; Erratum in *J. High Energy Phys.* **2013**, *10*, 52. [[CrossRef](#)]
71. Pontecorvo, B. Mesonium and anti-mesonium. *Sov. Phys. JETP* **1957**, *6*, 429.
72. Maki, Z.; Nakagawa, M.; Sakata, S. Remarks on the unified model of elementary particles. *Prog. Theor. Phys.* **1962**, *28*, 870. [[CrossRef](#)]
73. Wolfenstein, L. Neutrino Oscillations in Matter. *Phys. Rev. D* **1978**, *17*, 2369. [[CrossRef](#)]
74. Gribov, V.N.; Pontecorvo, B. Neutrino astronomy and lepton charge. *Phys. Lett. B* **1969**, *28*, 493–496. [[CrossRef](#)]
75. Mikheyev, S.P.; Smirnov, A.Y. Resonance Amplification of Oscillations in Matter and Spectroscopy of Solar Neutrinos. *Sov. J. Nucl. Phys.* **1985**, *42*, 913–917.
76. Aguilar-Arevalo, A.A.; Brown, B.C.; Conrad, J.M.; Dharmapalan, R.; Diaz, A.; Djuricic, Z.; Finley, D.A.; Ford, R.; Garvey, G.T.; Gollapinni, S. Updated MiniBooNE neutrino oscillation results with increased data and new background studies. *Phys. Rev. D* **2021**, *103*, 052002. [[CrossRef](#)]
77. Mueller, T.A.; Lhuillier, D.; Fallot, M.; Letourneau, A.; Cormon, S.; Fechner, M.; Giot, L.; Lasserre, T.; Martino, J.; Mention, G.; et al. Improved Predictions of Reactor Antineutrino Spectra. *Phys. Rev. C* **2011**, *83*, 054615. [[CrossRef](#)]
78. Huber, P. On the determination of anti-neutrino spectra from nuclear reactors. *Phys. Rev. C* **2011**, *84*, 024617. [[CrossRef](#)]
79. Giunti, C.; Laveder, M. Neutron oscillations. *Phys. Rev. D* **2008**, *77*, 093002. [[CrossRef](#)]
80. Aartsen, M.G.; Abbasi, R.; Ackermann, M.; Adams, J.; Aguilar, J.A.; Ahlers, M.; Ahrens, M.; Alispach, C.; Amin, N.M.; Andeen, K. eV-Scale Sterile Neutrino Search Using Eight Years of Atmospheric Muon Neutrino Data from the IceCube Neutrino Observatory. et al. *Phys. Rev. Lett.* **2020**, *125*, 141801. [[CrossRef](#)] [[PubMed](#)]
81. Abe, K.; Hagi, Y.; Hayato, Y.; Ikeda, M.; Iyogi, K.; Kameda, J.; Kishimoto, Y.; Marti, L.; Miura, M.; Moriyama, S. Solar Neutrino Measurements in Super-Kamiokande-IV. *Phys. Rev. D* **2016**, *94*, 052010. [[CrossRef](#)]
82. Gonzalez-Garcia, M.C.; Maltoni, M. Determination of matter potential from global analysis of neutrino oscillation data. *J. High Energy Phys.* **2013**, *1309*, 152. [[CrossRef](#)]
83. Maltoni, M.; Smirnov, A.Y. Solar neutrinos and neutrino physics. *Eur. Phys. J. A* **2016**, *52*, 87. [[CrossRef](#)]
84. Guzzo, M.M.; Masiero, A.; Petcov, S.T. On the MSW effect with massless neutrinos and no mixing in the vacuum. *Phys. Lett. B* **1991**, *260*, 154. [[CrossRef](#)]

85. Roulet, E. MSW effect with flavor changing neutrino interactions. *Phys. Rev. D* **1991**, *44*, 935. [[CrossRef](#)]
86. Yasuda, O. Neutrino oscillation phenomenology and the impact of Professor Masatoshi Koshihira. *Prog. Theor. Exp. Phys.* **2022**, *12*, 12B105. [[CrossRef](#)]
87. Alves, G.F.S.; Bertuzzo, E.; Salla, G.M. On-shell approach to neutrino oscillations. *Phys. Rev. D* **2022**, *106*, 036028. [[CrossRef](#)]
88. Banks, H.; Kelly, K.J.; McCullough, M. How broad is a neutrino. *J. High Energy Phys.* **2023**, *02*, 136. [[CrossRef](#)]
89. Bilenky, S.M. Flavor neutrino oscillations and time-energy uncertainty relation. *Phys. Scr. T* **2006**, *127*, 8. [[CrossRef](#)]
90. Bilenky, S.M.; von Feilitzsch, F.; Potzel, W. Neutrino Oscillations and Uncertainty Relations. *J. Phys. G* **2011**, *38*, 115002. [[CrossRef](#)]

Disclaimer/Publisher's Note: The statements, opinions and data contained in all publications are solely those of the individual author(s) and contributor(s) and not of MDPI and/or the editor(s). MDPI and/or the editor(s) disclaim responsibility for any injury to people or property resulting from any ideas, methods, instructions or products referred to in the content.